Original Research

Methods for Registration of Magnetic Resonance Images of Ex Vivo Prostate Specimens With Histology

Simon Y. Kimm, MD,[1] Tatum V. Tarin, MD,[1] Jin Hyung Lee, PhD,[2] Bob Hu, PhD,[2] Kristin Jensen, MD,[3] Dwight Nishimura, PhD,[2] and James D. Brooks, MD[1]*

Purpose: To evaluate two methods of scanning and tissue processing to achieve accurate magnetic resonance (MR)-histologic correlation in human prostate specimens.

Materials and Methods: Two prostates had acrylic paint markers injected to define the plane of imaging and serve as internal fiducials. Each was placed on a polycarbonate plane-finder device (PFD), which was adjusted to align the imaging and cutting planes. Three prostates were aligned by use of a plane finder key (PFK), a polycarbonate plate that locks the specimen in a cylindrical carrier. Markers were injected for registration analysis. Prostates were imaged, then sectioned. Imaging software was used to create registration maps of the MR and histology images. Measurements between control points were made and compared.

Results: Accurate correlation was achieved between MR and histologic images. The mean displacement (MD) between the corresponding registration points using the PFD technique ranged from 1.11–1.38 mm for each section. The MD for all sections was 1.24 mm. The MD using the PFK technique ranged from 0.79–1.01 mm for each section, and the MD across all sections for the PFK was 0.92 mm.

Conclusion: We describe two methods that can achieve accurate, reproducible correlation between MR imaging and histologic sections in human prostatectomy specimens.

Key Words: prostate; magnetic resonance imaging (MRI); histology; image registration; histologic correlation
J. Magn. Reson. Imaging 2012;36:206–212.

PROSTATE CANCER is the most common malignancy in males and constitutes the second most common cause of male cancer death (1). Currently, the diagnosis of prostate cancer is made through histologic examination of prostate tissue, obtained by biopsy or by surgery. To date, no imaging modality has been shown to reliably detect and diagnose the presence of prostate cancer (2). Magnetic resonance imaging (MRI), with its excellent soft-tissue discrimination, can provide high-resolution images of the prostate and surrounding tissues. Increased MRI field strengths, improved coil-detector arrays, and optimized scanning protocols continue to improve our ability to image the prostate at higher resolutions with improved signal-to-noise ratios (SNRs) (3). These advances promise to enhance our ability to detect small volume cancers.

To evaluate the ability of MRI to resolve prostate cancer, cross-sectional imaging must be correlated with pathologic findings. As MR image resolution routinely reaches submillimeter levels, the need for accurate registry with histology has become more acute. This is particularly important in prostate cancer, as many cases are discovered at small volumes and histologic grading of cancers can be carried out at relatively low resolution (2). MR-histologic correlation is difficult, as small differences in section angle, deformation during tissue fixation, and surgical distortion contribute to poor correlation. Traditional methods of prostate tissue processing (ie, serial step-sectioning) approximate the axial images produced by imaging by sectioning the prostate parallel to the prostate base (4). However, prior investigations have shown that this approach can produce a 5–15° difference in tissue angle between the base and apex of the prostate, with errors compounding with each section (5). As a result, histological correlation with MR images can be confounded.

To address the challenges in achieving accurate registry of histology with high-resolution MR images of the prostate, we developed two methods of scanning and tissue processing for use in ex vivo human prostate specimens. These methods could find application in developing high-resolution MRI approaches in prostate cancer visualization.

[1]Department of Urology, Stanford University, Stanford, California, USA.
[2]Department of Electrical Engineering, Stanford University, Stanford, California, USA.
[3]Department of Pathology, Palo Alto Veterans Affairs Health Care System, Palo Alto, California, USA.
Contract grant sponsor: Bio-X Interdisciplinary Initiatives Program, Stanford University.
*Address reprint requests to: J.D.B., Department of Urology, Room S287, Stanford University School of Medicine, 300 Pasteur Dr., Stanford, CA 94305-5118. E-mail: jdbrooks@stanford.edu
Received June 14, 2011; Accepted January 13, 2012.
DOI 10.1002/jmri.23614
View this article online at wileyonlinelibrary.com.

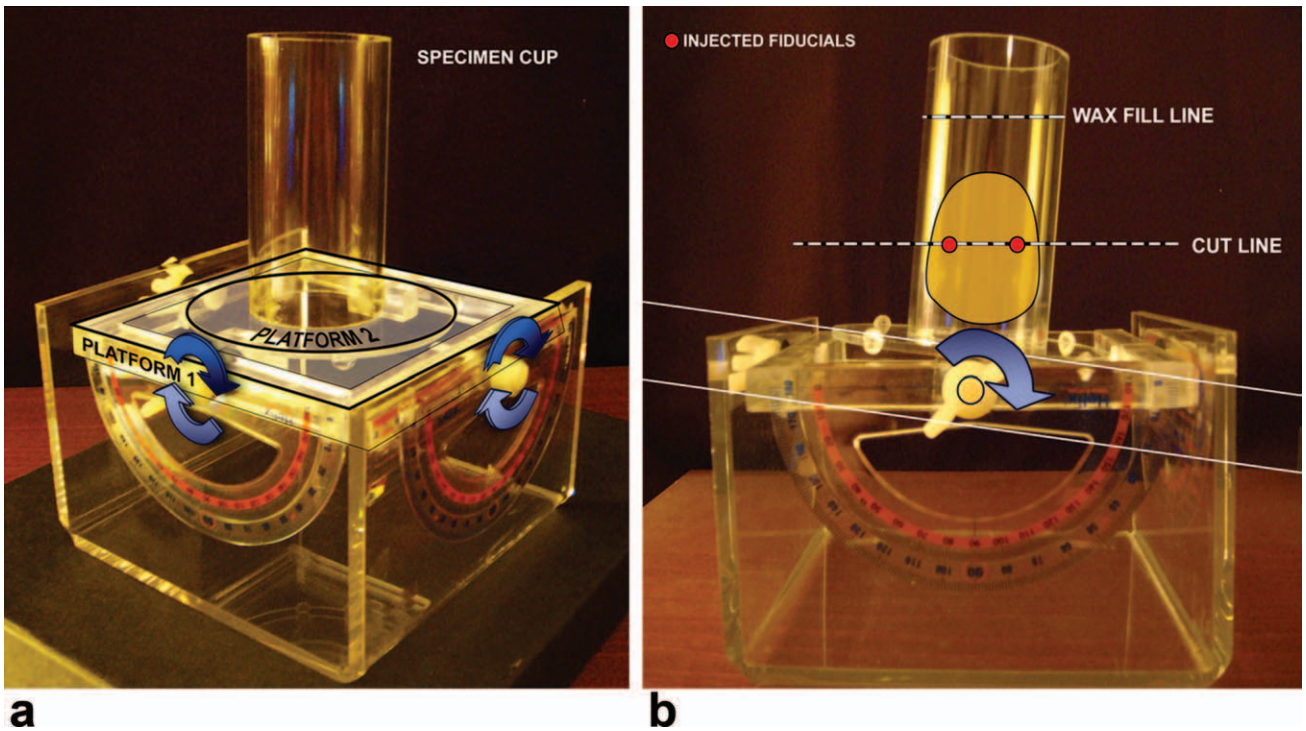

Figure 1. A plane finder device (PFD) is used to establish the imaging plane and has two platforms that can be rotated and tilted in the coronal and horizontal planes (**a**). After the injected fiducials are aligned, paraffin wax then establishes the cutting plane during histologic processing (**b**). [Color figure can be viewed in the online issue, which is available at wileyonlinelibrary.com.]

MATERIALS AND METHODS

Patients and Prostate Specimens

We obtained five human prostate specimens, with appropriate informed consent, after radical prostatectomy for prostate cancer. Institutional Review Board (IRB) approval for the use of human tissue was obtained. These specimens were procured immediately after surgery and kept in saline. Scanning of the specimens took place within hours of surgical removal. We used two methods of tissue registration. The first involved the use of a plane-finder device (PFD) and a second method involved the use of a plane-finder key (PFK).

Plane-Finder Device

To define the plane of imaging, a previously described technique of using injectable fluid acrylic paint markers as fiducials was utilized (6). Injected metallic acrylic paint is visible in histologic, gross, and MR sections, and is sufficiently viscid so as not diffuse once in the tissues. Three injections were made in the prostate, providing three points that defined a plane—a fiducial plane that serves as the plane of imaging and as the cutting plane when the specimen is later processed. Additional injections of fiducials were made in the prostate base and apex to aid in the registration process.

The specimen was placed on a polycarbonate platform that could be rotated in three dimensions, and adjusted to align the first set of fiducials in the horizontal imaging plane. Variations of this type of platform have been described, which serves as a PFD (Fig. 1) (4). This platform rotates and tilts along two axes to orient the specimen; it also holds the radiofrequency (RF) coil of the MRI scanner in place. The RF coil is positioned to surround the specimen carrier, perpendicular to the long axis of the prostate to maximize SNR.

The positions of the fiducials were determined in the axial, coronal, and sagittal planes by MRI prescan (Fig. 2). MRI prescanning produces lower-resolution images of a limited area with significantly reduced scanning times. The movable platform of the PFD was then tilted, with the goal of orienting the specimen such that the plane defined by the fiducials was parallel to the ground. After each adjustment the prescan process was repeated until the imaging plane was parallel to the scanning bed. Both prostates required three successive scans with adjustments to achieve alignment. The platform was locked in place and imaging performed according to the protocol outlined below. The chamber was later filled with paraffin wax, forming a meniscus that was parallel to the ground and therefore parallel to the plane of imaging. It is along this wax meniscus that the prostates were sectioned.

Plane-Finder Key

The PFK was designed to fit into the 6-cm coil cylinder of a Siemens 7T MRI research scanner, which has a bore size too small accommodate a PFD. The PFK consists of a polycarbonate plate $4 \times 1 \times 0.05$ cm in size. At each end are tabs that are placed into slots cut

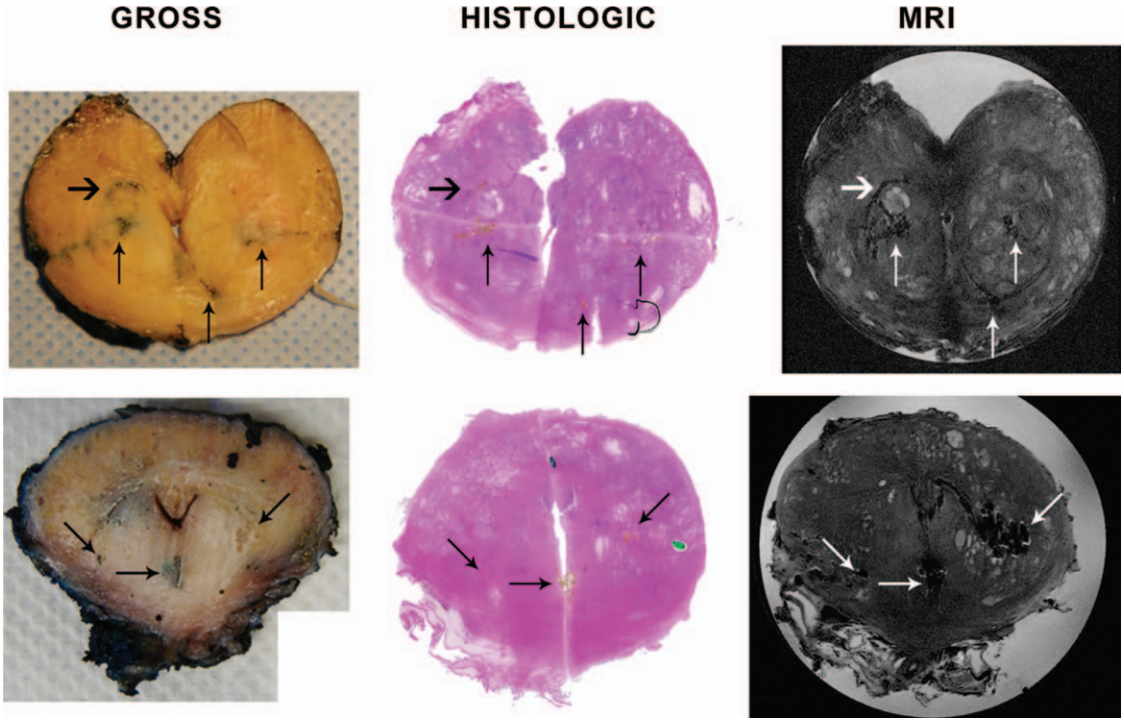

Figure 2. Injectable fiducials (arrows) are readily visualized in gross, histologic, and MRI sections providing key landmarks for histologic correlation.

into a polycarbonate cylinder. This cylinder houses the PFK and the specimen, with the PFK locked into the proper orientation. A central triangle (CT) of known area (0.433 cm^2) was cut out of the center of the PFK, which was used as a final check on specimen positioning during the scanning process. To define the plane of imaging, the PFK was inserted into the prostate (Fig. 3). Additional injections of fiducials were made in the prostate base and apex to aid in the evaluation of registration. The prostate-embedded key was locked into the specimen chamber. MRI prescanning was used to visualize the PFK. The plane created by the PFK was set as the imaging plane of the scanner. The region of interest (ROI) tool was used to mark the boundaries of the CT on axial imaging and the area was measured. Misalignment of the PFK and the imaging plane could be detected by differences in the measured area versus the known area of the CT. Where significant differences in area were measured (>5%), the imaging plane was redefined until there was good concordance between the values. With this technique there was no need for injection of fiducial

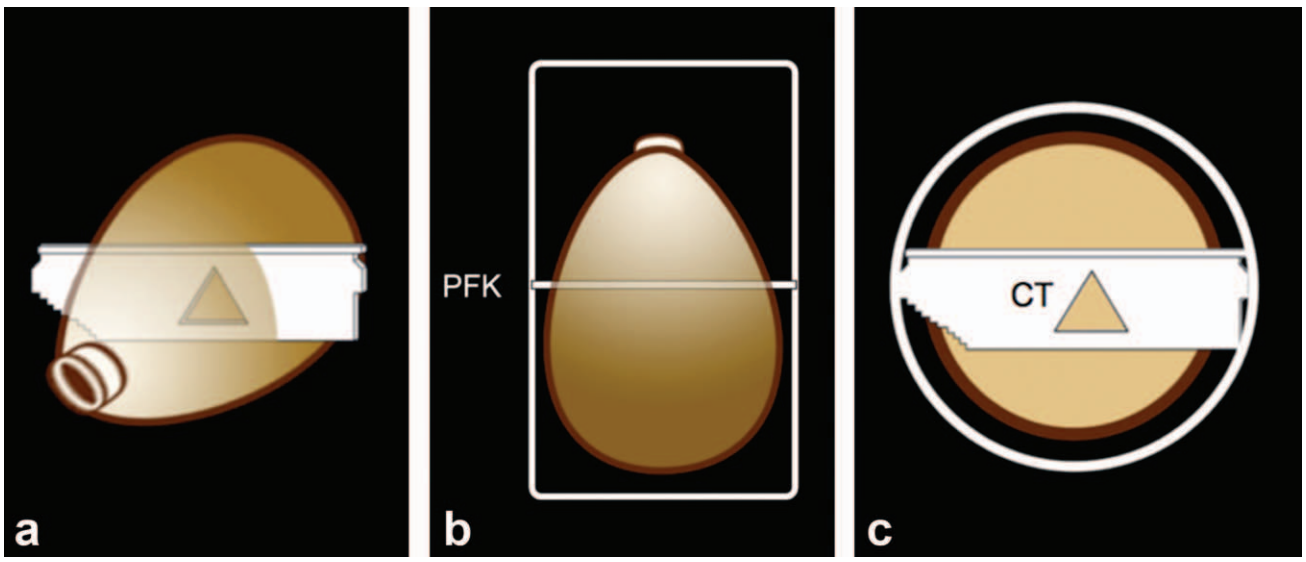

Figure 3. A plane finder key (PFK) is inserted into the prostate (**a**). The PFK locks into a nonmetallic carrier establishing the plane of imaging, and later the cutting plane (**b**, coronal view). A central triangle (CT) provides a reference area to improve the alignment of the planes (**c**, axial view).

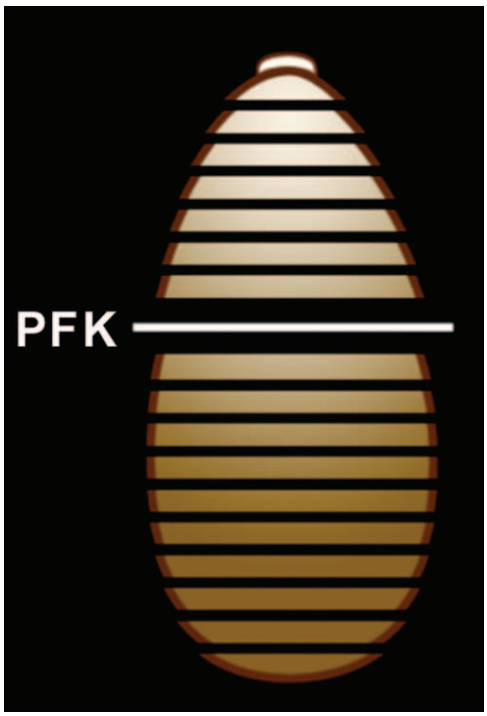

Figure 4. A plane finder key (PFK) establishes the cutting plane for step-sectioning of the prostate. A cutting jig is used to create sections parallel to the PFK. [Color figure can be viewed in the online issue, which is available at wileyonlinelibrary.com.]

markers since the plane could be oriented with the PFK device alone.

1.5T MRI

The prostates oriented in the PFD were imaged in a GE 1.5T EXCITE whole body scanner using a fast spin echo (FSE) protocol: TE = 130 msec, TR = 4750 msec, ETL = 18, BW = 15.63 kHz, 1 mm slice thickness, 50 slices, 4 NEX, 5.5 cm FOV, scan matrix 512, voxel dimensions (0.107 × 0.107 × 1.0 mm).

7T MRI

The prostates oriented with the PFK were imaged in a small bore Siemens 7T research scanner, using an FSE protocol: TE = 130 msec, TR = 4750 msec, ETL = 18, BW = 15.63 kHz, 0.5 mm slice thickness, 8.0 NEX, 5.5 cm FOV, scan matrix 512, voxel dimensions (0.107 × 0.107 × 0.5 mm). The MRI scans were performed with all image slices parallel to the PFK.

Tissue Fixation

After imaging, the tissue was fixed in formalin for 36 hours. We repeated the MRI after formalin fixation to confirm that the fiducial planes were unchanged. The areas of the peripheral zone, transition zone, central zone, and prostatic urethra were measured using the ROI tool in our imaging software (Osirix, Sunnyvale, CA). The overall change in volume after fixation was determined by fluid displacement before and after fixation. The specimen chamber of the PFD was filled with paraffin wax. After hardening, the meniscus of the wax was parallel to the imaging plane in the PFD (Fig. 1b) and used as the cutting plane.

Gross Pathologic Image Acquisition

A tissue-slicing apparatus was constructed from polycarbonate that included a tissue platform and a digital camera (D80, Nikon, Japan). The camera was fixed such that the focal axis of the camera was in alignment with the central axis of the wax-embedded specimen and photographs of the tissue face were taken in the plane of imaging. The camera position was calibrated by taking photographs of a standard flat test target with a rectilinear grid pattern.

Histologic Processing

For specimens scanned using the PFD, the wax-embedded tissue was sliced in the imaging plane at 3-mm intervals with an autopsy knife (Tissue-Tek Accu-Edge Semi-Disposable Autopsy Knife System, Sakura Finetek, Japan). The specimen was advanced in a Plexiglas carrier, which served as a cutting guide, and photographs were taken. For PFK specimens, the PFK was locked into the Plexiglas carrier and the first cut was made through the tissue cleavage plane created by the PFK. Serial 3-mm-step sections were then cut on a cutting jig, parallel to this plane (Fig. 4). This resulted in 7–9 slices for each prostate specimen.

Tissue slices were then prepared for histological processing. The remaining wax from each prostate step-section was removed and the tissue placed on a histology-mounting block. The tissue was dehydrated in a series of ethanol baths, treated with xylene, and paraffin used to create tissue blocks using standard tissue processing techniques. Five-μm-thick sections from the paraffin block were affixed to glass slides after staining with hematoxylin and eosin (H&E). Histology slides were digitized using a slide scanning system (Nikon, Japan) and saved as uncompressed TIFF files.

Evaluation of Registration

With imaging software (Osirix), the annotation cursor was used to create 10–25 registration points on each image. Sites such as anatomic landmarks and tissue boundaries were chosen. Corresponding points were placed on the scanned histology slides on landmarks that were clearly visible on both imaging and histology (Fig. 5). The center of a single registration mark was designated as the center (0,0) of a Cartesian coordinate system. Each registration mark was assigned a 2D coordinate value (x,y) relative to the mark defined as the center. Distances between the registration marks were measured using imaging software (Adobe Systems, San Jose, CA). Point-to-point distances were measured from the center point to each registration mark on each MR image. A similar process was used to measure the distance of each point to the center on each histologic image. For each slice, three different center points were used and the distances measured. We compared the distances measured between the

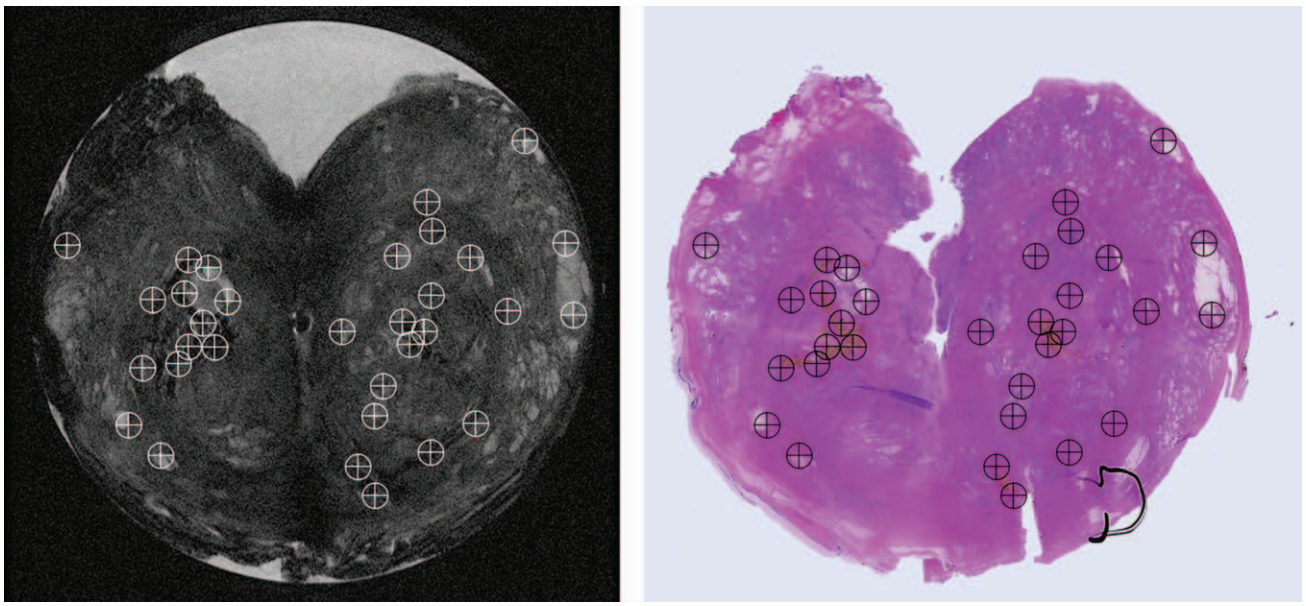

Figure 5. Manual placement of registration marks on fiducials, anatomic boundaries, and landmarks are used in displacement analysis, MRI left, H&E stained slide right. [Color figure can be viewed in the online issue, which is available at wileyonlinelibrary.com.]

MR images and histology images (Fig. 5). The difference between the measured distance of a registration mark on the MR image and the corresponding distance on the histologic image was calculated. The mean of all the differences were calculated to obtain the MD for each slice.

RESULTS

Our objective was to develop methods for precise registration of MR images with histology of ex vivo prostate specimens. Recently, Rouvière et al (6) described the use of acrylic-based inorganic paint as fiducial markers for histologic correlations. These fiducials are visible on MR as susceptibility artifacts and can be seen on gross and microscopic tissue analysis (Fig. 2). They do not cause tissue reaction, they remain stable during tissue fixation, and, when used in combination with the PFD, the imaging plane can be defined. We adapted the PFD for use in the prostate. A specimen carrier of a size appropriate to the prostate gland was selected and the RF coil was placed to maximize SNR. Excellent correlation was achieved between MR, histologic, and gross anatomic images. Injected markers were visible in consistent positions across sections for the PFD technique (Fig. 2). The mean difference between the corresponding registration points using the PFD technique ranged from 1.11–1.38 mm for each section (Table 1). The MD across all sections for the PFD was 1.24 mm. These compare favorably with the in-plane MR voxel dimension. Excellent registration accuracy of MR, tissue, and histology images is clearly evident, with good correspondence of fiducial markers. Results were similar across adjacent tissue slices, with less displacement in sections with visible fiducial markers or the PFK.

One limitation of the PFD was that it could only be used in conjunction with our clinical 1.5T MRI scanner, which provided less anatomic detail than the higher field strength MRI scanner. The PFK was developed because the small bore of the 7T MRI coil could not accommodate a PFD. Its size and shape is ideal for use in ex vivo human prostates. An aperture of known area (CT, Fig. 3c) was created in the PFK as an additional internal check on plane alignment. Prior studies have quantified the mean changes in a fixed area induced by 0–3 mm anterior/posterior translations and 0–6° superior/inferior and right/left rotation. Small rotations and translations resulted in substantial changes in the CT area (4). The imaging plane was set and an MRI prescan was performed that ensured a precise CT area.

Table 1
Plane Finder Device Mean Displacement Measurements in Millimeters

PFD 1	MD (mm)	PFD 2	MD (mm)
1	2.20	1	0.69*
2	1.10*	2	0.79*
3	1.30	3	0.81
4	0.67*	4	1.25*
5	0.84	5	2.11
6	0.26*	6	1.22*
7	1.48	7	2.76
8	0.99*		
9	1.12*		
	1.11		1.38

PFD1 and PFD2 represent two different prostates. Each number represents a histologic section from the prostatic apex to the base, with MD representing the mean difference in measurement between registration points on the MRI scan and histology image. The MD across all sections was 1.24 mm. An asterisk (*) indicates the presence in injected fiducials. PFD, plane finder device; MD, mean displacement; MRI, magnetic resonance imaging.

Table 2
Plane Finder Key Mean Displacement Measurements in Millimeters

PFK 1	MD (mm)	PFK 2	MD (mm)	PFK 3	MD (mm)
1	1.22	1	2.00	1	0.93*
2	1.17	2	1.30*	2	1.17
3	0.91*	3	0.30	3	0.89
4	0.46	4	0.37+	4	0.66+
5	0.24+	5	0.94	5	1.24
6	0.36*	6	1.40	6	0.77*
7	0.33*	7	0.74*	7	0.89*
8	1.39			8	1.10
9	1.03				
mean	0.79	mean	1.01	mean	0.96

PFK 1, PFK 2, and PFK 3 represent three different prostate specimens. Each number represents a histologic section from the prostatic apex to the base, with MD representing the mean difference in measurement between registration points on the MRI scan and histology image. A plus sign (+) indicates the presence of the PFK. An asterisk (*) indicates the presence in injected fiducials. PFK, plane finder key; MD, mean displacement; MRI, magnetic resonance imaging.

The registration accuracy for each prostate section using the PFK technique is summarized in Table 2. For the three prostate specimens using this technique, MD between the corresponding registration points between histology and imaging ranged from 0.79–1.01 mm for each section. The MD across all sections for the PFK was 0.92 mm. Analyses of the mean displacements reveal that tissue sections in closest proximity to the injected fiducials or PFK showed the greatest degree of correlation.

DISCUSSION

Intensive application of prostate-specific antigen (PSA) screening over the past three decades has been associated with a decrease in prostate cancer size and decrease in prostate cancer stage (7). Furthermore, prostate cancers tend to infiltrate normal prostate tissues with resulting irregular borders, in contrast with most other malignancies, which usually form discrete tumors that displace normal tissues. By necessity, future imaging strategies will need to provide relatively high-resolution views of prostate cancers to be of clinical utility for prostate cancer diagnosis and therapy. Therefore, methods for precise alignment of MR images with histology will be critical in developing high-resolution approaches. We describe two complementary approaches for precise registry of MR images with histology.

The PFD results in precise alignment of gross, microscopic, and MR images. It combines a method of specimen alignment, scanning, and tissue processing that produces consistent results with good accuracy. The device is easy to construct and provides a method for accurate alignment of imaging and specimen cutting planes. In contrast with the PFK, it does not require perforation of the specimen and thereby preserves the contour of the prostate as well as the external capsule of the gland, which is important in pathological assessment of the prostate for cancer extension outside of the capsule, which is important in clinical assessment.

The PFD does have some shortcomings. Because of its size, the PFD could only be used in conjunction with a clinical MRI scanner, which provided much less anatomic detail than the higher field strength afforded by a small bore research MRI scanner. This made placement of clearly corresponding control points more difficult. In addition, the PFD requires placement of fiducial markers in the prostate, and there is a learning curve to placing these markers uniformly. Furthermore, applied fiducials can often develop irregular borders and this contributes to measurement error.

The PFK was developed to accommodate the small bore of the 7T MRI coil and represents a novel method for registry of gross and histologic cross-sections with MR images. Its size and shape is ideal for use in ex vivo human prostate, and our results show that excellent correlations can be achieved when it is used to simultaneously define the imaging and cutting planes. In contrast with the PFD, the PFK is simple in its design and easier to deploy, and does not require the use of injected fiducials as landmarks for imaging plane acquisition. In addition, the plane of imaging was more easily defined with PFK since it is essentially a 2D plate, unlike three fiducial points that must be aligned in 3D space.

Our methodology for assessing registration accuracy required the use of injected fiducial markers and the manual identification of internal landmarks in the prostate. In the PFD, three injected fiducials placed in the mid-prostate served to identify the imaging and cutting plane. No fiducials were used to establish this plane in the prostates utilizing the PFK. Additional injections were made in clusters in the apex and base of the prostate in both techniques, and were important in confirming the registration of the slices in which they appeared. In addition to use of these fiducials, we used measurements between internal landmarks that would assess both in-slice deformations and tissue slicing that did not align with the plane of imaging. Multiple control points with a mix of landmark types were used. The prostate is not a radiographically or histologically homogenous organ, and numerous landmarks could be identified that aided in confirming slice registration. Stromal septations course in multiple directions within the prostate, defining the zonal anatomy of the gland. Internal stromal nodules also provide spherical boundaries. Measurements between these types of identifiable structures diverge and converge with each step-section and aid in the identification of misregistered sections. In addition, prostatic calcifications, microcysts, and ellipsoid glandular structures often serve a similar function as the injected fiducials. This added to our confidence that sections were registered correctly. Correlation and placement of control points is a manual process, however, and depends on the proper identification of clear anatomic landmarks. For both the PFK and PFD, the most accurate correlations occurred in the prostate slices that were near or

included fiducials or the PFK. Registration accuracy degraded in slices without them, worsening with slices further away. We surmise that this is because translational and rotational misalignments are minimized where multiple fiducials and the PFK are visible, and misregistrations are more likely when only internal landmarks are used. We feel that the MD measurements help to quantify these misalignments, although this measure is insensitive to the type of transformation contributing to the misalignment.

When comparing the PFD with the PFK, we found that the PFK was ideal for use in high field strength MRI scanners by virtue of its size. The plane of imaging was easy to define given the dimensions of the PFK, and the sectioning process with the PFK eliminated the need for embedding the specimen in paraffin wax.

As expected, the 7T MRI protocol produced superior images of the prostate at higher resolution compared with the 1.5T MRI protocol with favorable SNR. Despite significantly longer scanning times, the anatomic detail produced by the 7T MRI made control point placement easier and more precise.

This investigation has several limitations. Manual registration of control points can be prone to error, as it depends on internal anatomic landmarks of the prostate, which can be highly variable and inconsistent. In this study, a single investigator placed the control points and made the measurements, so no comment can be made about interobserver variability. In addition, measurements in tissue sections further away from fiducial markers or a PFK can show greater variance between landmarks because small errors in alignment are compounded. Furthermore, fixation shrinkage and surgical distortion can compound this variability. Our volumetric data show an ≈4%–8% shrinkage of the tissue after formalin fixation, consistent with shrinkage artifacts reported previously (4). Area measurements of prostatic zones from MRI before and after fixation show that fixation shrinkage affects the exterior of the prostate more than the interior, usually 5–10 mm from the prostatic capsule. Therefore, we avoided using exterior landmarks. We found that the relative internal distances between internal structures was preserved after fixation. For this reason, we opted not use distortion-correcting warping transformations in our histology images, which typically rely on outer boundary registration points.

Finally, these methods were performed on a limited number of specimens, and further study and refinement of technique will be required in other applications of prostate imaging. In the future, more sophisticated boundary detection and image processing algorithms may be utilized to standardize image registration (8). Development of the PFD and PFK also provides an opportunity for further refinement in our MRI scanning protocols to improve our ability to visualize malignancy.

In conclusion, accurate, reproducible correlation can be achieved between MRI, gross anatomic sections, and histologic sections in human prostatectomy specimens by use of a PFD with injected acrylic paint fiducials, or a PFK and cutting jig. Use of a PFK allowed greater flexibility in its use because of its simplicity and small size.

REFERENCES

1. Dennis LK, Resnick MI. Analysis of recent trends in prostate cancer incidence and mortality. Prostate 2000;42:247–252.
2. Carter B, Partin AW. Diagnosis and staging of prostate cancer. In: Wein AJ, Kavoussi LR, Novick AC, Partin AW, Peters CA, editors. Campbell-Walsh urology, 9th ed. Philadelphia: Saunders, Elsevier; 2007.
3. Beyersdorff D, Taymoorian K, Knosel T, et al. MRI of prostate cancer at 1.5 and 3.0 T: comparison of image quality in tumor detection and staging. Am J Roentgenol 2005;185:1214–1220.
4. Rouvière O, Reynolds C, Hulshizer T, et al. MR histological correlation: a method for cutting specimens along the imaging plane in animal or ex vivo experiments. J Magn Reson Imaging 2006;23: 60–69.
5. Jager G, Ruijter E, van de Kaa C, et al. Local staging of prostate cancer with endorectal MR imaging: correlation with histopathology. Am J Roentgenol 1996;166:845–852.
6. Rouvière O, Reynolds C, Le Y, et al. Fiducial markers for MR histological correlation in ex vivo or short-term in vivo animal experiments: a screening study. J Magn Reson Imaging 2006;23:50–59.
7. Galper SL, Chen M-H, Catalona WJ, Roehl KA, Richie JP, D'Amico AV. Evidence to support a continued stage migration and decrease in prostate cancer specific mortality. J Urol 2006;175:907–912.
8. Breen M, Lazebnik R, Wilson D. Three-dimensional registration of magnetic resonance image data to histological sections with model-based evaluation. Ann Biomed Eng 2005;33:1100–1112.